

GEAR: Graph-Evolving Aware Data Arranger to Enhance the Performance of Traversing Evolving Graphs on SCM

Wen-Yi Wang, Chun-Feng Wu¹, *Member, IEEE*, Yun-Chih Chen², *Member, IEEE*,
Tei-Wei Kuo³, *Fellow, IEEE*, and Yuan-Hao Chang⁴, *Fellow, IEEE*

I. INTRODUCTION

Abstract—In the era of big data, social network services continuously modify social connections, leading to dynamic and evolving graph data structures. These evolving graphs, vital for representing social relationships, pose significant memory challenges as they grow over time. To address this, storage-class memory (SCM) emerges as a cost-effective solution alongside DRAM. However, contemporary graph evolution processes often scatter neighboring vertices across multiple pages, causing weak graph spatial locality and high-TLB misses during traversals. This article introduces SCM-Based graph-evolving aware data arranger (GEAR), a joint management middleware optimizing data arrangement on SCMs to enhance graph traversal efficiency. SCM-based GEAR comprises multilevel page allocation, locality-aware data placement, and dual-granularity wear leveling techniques. Multilevel page allocation prevents scattering of neighbor vertices relying on managing each page in a finer-granularity, while locality-aware data placement reserves space for future updates, maintaining strong graph spatial locality. The dual-granularity wear leveler evenly distributes updates across SCM pages with considering graph traversing characteristics. Evaluation results demonstrate SCM-based GEAR's superiority, achieving 23% to 70% reduction in traversal time compared to state-of-the-art frameworks.

Index Terms—Checkpointing, evolving graph, graph, HW/SW Co-design, memory management, middleware, non-volatile memory, system software.

Manuscript received 4 August 2024; accepted 4 August 2024. This work was supported in part by the National Science and Technology Council under Grant 113-2628-E-A49-021, Grant 112-2222-E-A49-002-MY2, Grant 113-2223-E-001-001, Grant 111-2221-E-001-013-MY3, Grant 113-2927-I-001-502, and Grant 111-2923-E-002-014-MY3; in part by the Academia Sinica under Grant AS-IA-111-M01; and in part by the Ministry of Education under Yushan Young Fellow Program. This article was presented in the International Conference on 2024 and appears as part of the ESWEEK-TCAD special issue. This article was recommended by Associate Editor S. Dailey. (*Corresponding authors: Chun-Feng Wu; Yuan-Hao Chang.*)

Wen-Yi Wang is with the Department of Computer Science and Information Engineering, National Taiwan University, Taipei 106, Taiwan (e-mail: r09922090@ntu.edu.tw).

Chun-Feng Wu is with the Department of Computer Science, National Yang Ming Chiao Tung University, Hsinchu 300, Taiwan (e-mail: cfwu417@cs.nycu.edu.tw).

Yun-Chih Chen is with the Department of Computer Science, Technische Universität Dortmund, 44227 Dortmund, Germany (e-mail: yunchih.chen@tu-dortmund.de).

Tei-Wei Kuo is with the Delta Electronics, Department of Computer Science and Information Engineering, High Performance and Scientific Computing Center, and the Center of Data Intelligence: Technologies, Applications, and Systems, National Taiwan University, Taipei 10617, Taiwan (e-mail: ktw@csie.ntu.edu.tw).

Yuan-Hao Chang is with the Institute of Information Science, Academia Sinica, Taipei 115, Taiwan (e-mail: johnson@iis.sinica.edu.tw).

Digital Object Identifier 10.1109/TCAD.2024.3447222

SOCIAL network services utilize graph data structures to manage the connections between users. The relationship is highly dynamic, with connections added, updated, or removed at all times [1], [2]. As a result, the underlying graph data structures are dynamic and change with time. These dynamic graphs are known as evolving graphs: the connection between any two users may not be static all the time [3]. As evolving graphs grow over time, so does the system's memory demand. Storage-class memory (SCM) [4], [5], [6], [7] can augment DRAM to provide larger memory space at a lower price, alleviating the need to constantly add more DRAM to meet memory demand. Recent works in graph processing propose to buffer graph updates in RAM before flushing them to SCMs in batch [8], [9]. Our investigation reveals that such batch updates can be inefficient, with vertice updates spread across multiple batches and neighboring vertices spread across multiple pages. As a result, this characteristic leads to weak graph spatial locality, which may result in high-translation lookaside buffer (TLB) misses during subsequent graph traversals. To improve graph traversing performance, this work proposes a joint management middleware that take graph spatial locality into account in the data placement policy on SCMs.

Major social network providers, such as Google [10], Meta [11], and JingDong (JD.com) [2], have adopted graph processing algorithms, such as page rank and graph neural networks, to extract information from Web pages and social networks. A distributed system is one option for storing all graph data in memory. However, building an efficient distributed system remains a challenge, especially for small companies, due to high deployment and maintenance costs, load balancing, and fault tolerance. Out-of-core systems are alternative architectures that run graph processing on a single consumer-level machine, supplementing limited memory capacity with storage devices. Graph processing system based on out-of-core architecture have gained significant attention in the community [12], [13]. GraphChi [14] proposed breaking down large graphs into small parts and storing them in storage devices. Several works (e.g., FlashGraph [15], Graphene [16], and GraphSSD [17]) have proposed to carefully manage Solid-State Drives by adopting some I/O request merging or sophisticated buffering approaches with considering graph access behaviors. In contrast to processing static graphs,

70 these systems need a new data structure to track the most
 71 recent version of each vertex and edge in evolving graphs.
 72 Section II will provide a comprehensive overview of cutting-
 73 edge solutions and challenges.

74 However, we observed that state-of-the-art evolving graph
 75 frameworks have poor graph spatial locality, which makes
 76 them inefficient in executing graph traversal algorithms. We
 77 proposed a joint management middleware between graph-
 78 evolving processing and memory devices (including both
 79 DRAM and SCMs), called the SCM-Based Graph-Evolving
 80 Aware Data ArrangeR (GEAR). Our goal is to arrange and
 81 write the evolving graph data into SCMs while achieving
 82 strong graph spatial locality. The SCM-Based GEAR has three
 83 major components: 1) multilevel page allocation; 2) locality-
 84 aware data placement; and 3) a dual-granularity wear leveler.

- 85 1) The main idea behind multilevel page allocation is
 86 to prevent graph-evolving processes from scattering
 87 neighbor vertices across different pages. Technically, the
 88 system maintains multilevel size subpages and assigns
 89 a suitable-size subpage to accommodate all neighbors
 90 associated with each vertex, taking into account their
 91 number.
- 92 2) The locality-aware data placement reserves an unused
 93 area in each subpage for future graph updates to the cor-
 94 responding vertex, ensuring strong graph spatial locality
 95 even as the graph evolves over time.
- 96 3) The dual-granularity wear leveler, in conjunction with
 97 our page allocation, distributes graph updates evenly
 98 across all memory pages on SCM during graph evolu-
 99 tion. The evaluation results show that, compared to
 100 the state-of-the-art frameworks, our SCM-based GEAR
 101 can save the total execution time by 23%–70% when
 102 traversing an evolving graph.

103 The remainder of this article is organized as follows.
 104 Section II elaborates the graph evolving processes and shows
 105 the impact of the weak graph spatial locality on the graph
 106 traversal time. Section III provides the design concept and
 107 implementation of the SCM-based GEAR. Section IV evalu-
 108 ates the proposed strategy. Finally, Section V concludes this
 109 article.

110 II. BACKGROUND, OBSERVATION, AND MOTIVATION

111 A. Background

112 1) *Evolving Graphs*: Graphs are commonly used to repre-
 113 sent the relationship between data points. In general, each node
 114 in a graph represents a data point, and the edge that connects
 115 two data points (or nodes) records their relationship. A graph
 116 is considered a *evolving graph* if its layout or edge weights
 117 change over time. Social networks, for example, are constantly
 118 evolving [18], [19] as new users join and connections are
 119 established frequently. To analyze an evolving graph over
 120 time, evolving graph processing systems take snapshots on
 121 a regular basis [20]. However, systems storing multiple full
 122 snapshots¹ may waste huge memory space to accommodate
 123 redundant data. Modern graph processing frameworks, like

¹A full snapshot is a snapshot, which contains the entire graph layout in the moment of taking snapshot.

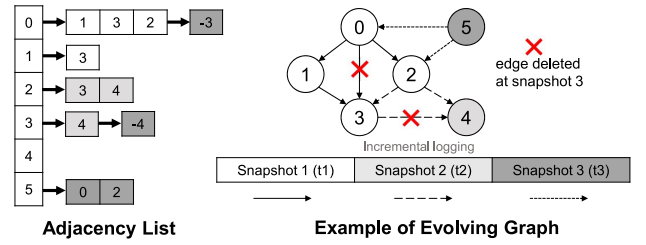


Fig. 1. Data structure for evolving graphs.

LLAMA [21], use *delta snapshot* [22] to save memory
 space by storing only the updated nodes or edges in each
 snapshot. In other words, each delta snapshot only contains
 graph updates (e.g., insertion, modification, and deletion) that
 occurred after the previous delta snapshot, so all snapshots
 must be read to traverse the entire graph. With support for
 delta snapshots, evolving graph processing systems can not
 only provide version control but also efficiently analyze graphs
 in the time domain. In the rest of this article, “delta snapshot”
 and “snapshot” are used interchangeably.

An evolving graph is typically stored in the format of an
 adjacency list [23], which is also applied to static graphs. An
 adjacency list maintains a linked list for each vertex to chain all
 correlated neighbors, and all updates from the same snapshot
 are grouped in an array [20]. Its structures enables efficient
 traversal all neighbors of any vertex in the adjacency list.
 Fig. 1 shows an evolving graph and its adjacency list format.
 The graph evolves to its third snapshot. The first snapshot
 includes four insertions (i.e., (1, 3), (0, 3), (0, 1), and (0, 2),
 with (1, 3) representing the newly inserted edge connecting
 vertex 1 and 3. The second snapshot contains three insertions,
 while the third snapshot has two insertions and two deletions.
 It is worth noting that, in the evolving graph framework,
 deleting an edge is typically translated into out-place updates.
 Rather than removing the deleted edge directly, we create a
 new edge with a negative sign. Out-place update not only
 lowers the cost of fine-grained memory modification, but it
 also makes it simple to go back to a previous version of the
 evolving graph.

2) *Storage Class Memory*: As the graph continues to
 evolve over time, the sheer volume of data within the graph
 structure increases proportionally, leading to more frequent
 and intensive data movements within systems. This growth in
 data size poses significant challenges for memory management
 and access efficiency [24]. Fortunately, recent advancements
 in manufacturing technologies, such as 3-D X-point [25],
 [26], [27], [28] and ultralow-latency NAND Flash [29], [30],
 [31], [32]), have paved the way for the emergence of
 SCM [33], [34]. These innovative memory solutions offer a
 hybrid approach, combining the speed and byte-addressable
 access of DRAM with the nonvolatility and higher density
 of traditional storage devices. Several products and proto-
 types have emerged to capitalize on these advancements,
 including Intel® Optane™ Persistent Memory [35] and HPE
 NVDIMM [6], [36].

SCM represents a new category of memory devices that
 combine the desirable characteristics of both DRAM and
 traditional storage devices. These memory devices offer

172 byte-addressable access granularity with 64-B cacheline
 173 accesses, ensuring efficient data retrieval and manipulation.
 174 Additionally, SCMs feature nonvolatility, allowing data to be
 175 retained even when power is removed, akin to storage devices.
 176 Moreover, SCMs boast lower-unit costs (price/GB) compared
 177 to DRAM and higher-storage density, providing up to 512-GB
 178 per DIMM, making them an attractive solution for memory-
 179 intensive applications [37].

180 Moreover, the integration of SCM into computing systems
 181 has been further facilitated by its diverse connectivity options.
 182 In addition to occupying traditional DIMM channels, SCM can
 183 also be connected via PCIe channels, leveraging the compute
 184 express link (CXL) interconnection² [38], [39], [40], [41].
 185 This flexibility in connectivity enables SCM to be seamlessly
 186 integrated into existing architectures, offering greater scalabil-
 187 ity and adaptability to evolving memory requirements. With
 188 SCM’s ability to bridge the gap between DRAM and storage,
 189 computing systems can achieve enhanced performance and
 190 efficiency in handling the growing demands of evolving graph
 191 structures and other data-intensive workloads.

192 However, due to their slower performance and shorter
 193 lifespan relative to DRAM, SCMs are typically utilized
 194 as extensions of DRAM rather than as direct replace-
 195 ments [42], [43]. In this hierarchical memory architecture,
 196 frequently accessed data (such as inner nodes in tree-data
 197 structure) resides in DRAM to leverage its faster access times
 198 and lower latency [42]. Conversely, less frequently accessed
 199 or large-scale data (such as leaf nodes in tree-data structure)
 200 that exceeds DRAM capacity is stored in SCMs, allowing
 201 for efficient use of available memory resources. One notable
 202 advantage of SCMs is their direct accessibility by CPUs,
 203 enabling seamless data transfer from SCMs directly into the
 204 CPU cache in cacheline-sized chunks. This direct access
 205 capability, discussed extensively in prior research [4], [44],
 206 allows for efficient utilization of SCMs alongside DRAM,
 207 mitigating the performance impact of slower SCM access
 208 times by leveraging CPU cache mechanisms. As a result, SCM
 209 adoption offers promising opportunities for improving memory
 210 performance and scalability in modern computing systems.

211 B. Observation

212 1) *Delta Snapshots Break Graph Spatial Locality*: Delta
 213 snapshots can generate multiple data versions for the same
 214 graph, significantly increasing memory usage and necessi-
 215 tating larger memory devices. Another major problem with
 216 delta snapshots is a loss of spatial locality. As more snap-
 217 shots are generated, neighboring vertices are scattered across
 218 multiple memory pages, significantly degrading graph traversal
 219 performance. In many graph processing algorithms, when a
 220 vertex is accessed, all of its 1-hop neighbor vertices are also
 221 accessed. Because these neighbors are updated at different
 222 times, they are stored on separate memory pages. Many
 223 graph processing frameworks write snapshots to pages in
 224 chronological order (i.e., by creation time). As a result, vertices

²CXL is a high-speed interconnect technology that facilitates efficient communication between CPUs and accelerators, including memory devices, to enable heterogeneous computing architectures.

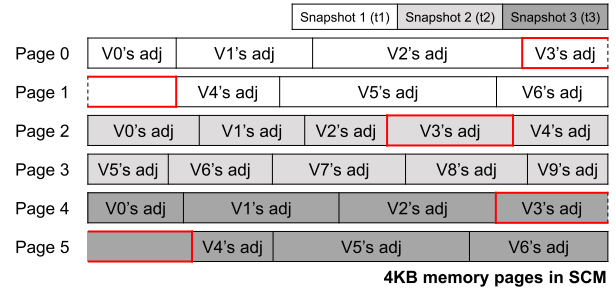


Fig. 2. Storing evolving graph on memory.

225 physically stored together may be logically distant from one
 226 another. Consequently, compared to ideal placement, more
 227 pages have to be read in a graph traversal to access each
 228 vertex’s neighbors, resulting in extra page table walks and TLB
 229 accesses.

230 Fig. 2 shows an example to illustrate the impact of graph
 231 spatial locality. Each rectangle represents a 4-kB page, where
 232 different gray levels indicate different snapshots. For example,
 233 the darkest part implies all graph updates belonging to the
 234 third snapshot. Besides, adj stands for an adjacency list, where
 235 V0’s adj means the adjacency list of V0. Assuming that
 236 neighbor vertices belonging to V3 evolves during different
 237 time period (e.g., t_1 , t_2 , and t_3), those updated neighbor
 238 vertices are scattered across three snapshots. In this case, it
 239 requires 5 page accesses (marked by red lines) to explore
 240 V3’s neighbors, where each page access might cause 1 TLB
 241 access and at most 4 memory accesses for walking page
 242 tables. Even worse, the performance degradation becomes
 243 more serious where systems shall explore most of the vertices
 244 for traversing a graph, instead of exploring only one vertex.
 245 Although some frameworks, such as LLAMA, can alleviate
 246 the performance impact by periodically merging multiple snap-
 247 shots, the performance of graph traversing becomes unstable
 248 and fluctuates seriously. The reason is that, the graph traversing
 249 reaches best performance right after running snapshots merg-
 250 ing, but it becomes worse until triggering the next merging.

251 Fig. 2 demonstrates the impact of graph spatial locality.
 252 Each rectangle represents a 4-kB page, and the different
 253 gray levels indicate different snapshots. For example, the
 254 darkest part denotes all graph updates for the third snapshot.
 255 Furthermore, “adj” stands for an adjacency list, and “V0’s adj”
 256 denotes V0’s adjacency list. Assuming that neighbor vertices
 257 in V3 evolve over different time periods (e.g., t_1 , t_2 , and
 258 t_3), the updated neighbor vertices are distributed across three
 259 snapshots. In this case, it takes 5 page accesses (marked by
 260 red lines) to traverse V3’s neighbors, with each page access
 261 potentially resulting in 1 TLB access and up to 4 memory
 262 accesses for walking page tables. Even worse, performance
 263 degradation worsens when systems must traverse all of the
 264 vertices in order to traverse a graph, rather than just one.
 265 Although some frameworks, such as LLAMA, can mitigate the
 266 performance impact by periodically merging multiple snap-
 267 shots, graph traversal performance still fluctuates significantly:
 268 traversal performs best immediately after a snapshot merge,
 269 but gradually degrades thereafter.

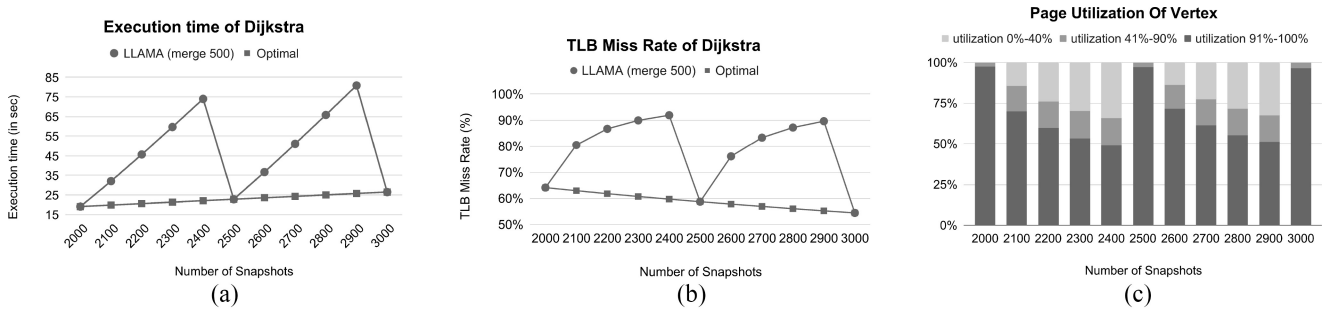


Fig. 3. Weak graph spatial locality hurts performance (Dataset: Friendster). (a) Execution time. (b) TLB miss rate. (c) Page utilization.

270 2) *Performance Impact Under Weak Graph Spatial*
 271 *Locality*: We conducted a series of experiments to validate
 272 our findings. Fig. 3 shows the performance results. We use
 273 LLAMA [21] as an example, which is a representative
 274 evolving graph framework. Without loss of generality, the
 275 LLAMA merge frequency is set to every 500 snapshots. To
 276 simulate graph evolution, we divide a large graph, Friendster,³
 277 into 10000 snapshots, and the graph will eventually evolve
 278 (or update) 10000 times. We evaluated graph traversal
 279 performance by running the Dijkstra algorithm every 100 snap-
 280 shots using two approaches. The first approach is LLAMA,
 281 which stores snapshots in SCMs. The second approach is
 282 called “optimal.” It merges all snapshots in DRAM and
 283 immediately rewrite a new graph to SCMs. This approach has
 284 the strongest spatial locality but can suffer from high-update
 285 overhead.

286 Fig. 3(a) and (b) show evaluation results for overall exe-
 287 cution time and TLB miss rate, respectively. The x -axis in
 288 both figures represents the number of archived snapshots.
 289 Fig. 3(a) shows that the placement issue may significantly
 290 affect the execution time, with the system adopting LLAMA
 291 spending 5 times more execution time than the system running
 292 the optimal approach. Running LLAMA breaks graph spatial
 293 locality, causing the CPU to read extra pages, resulting in
 294 high-TLB misses and frequent page table walks, as shown in
 295 Fig. 3(b). Furthermore, it is obvious that the performance of
 296 running graph traversal is unstable when using LLAMA. This
 297 unstable performance will degrade the user experience. Even
 298 worse, frequently merging snapshots may result in frequent
 299 access to SCMs, which consumes additional energy.

300 The above experiment shows that weak graph spatial local-
 301 ity can reduce page utilization. The page utilization of each
 302 vertex is defined as the ideal memory size occupied by the
 303 vertex’s neighbors divided by the memory size occupied by
 304 the vertex’s neighbors. For example, the total size of V1’s
 305 adjacency list (i.e., all of V1’s neighbors) is less than the
 306 size of one page, requiring only one memory page to store it.
 307 In reality, V1’s page utilization is less than 10% because its
 308 neighbors are scattered across 10 memory pages.

309 Fig. 3(c) shows page utilization for a system with varying
 310 snapshots. The x -axis shows the number of snapshots owned
 311 by the system, while the y -axis shows page utilization across
 312 all vertices. To better demonstrate the trend, we divide page
 313 utilization into three categories: 1) 0%–40%; 2) 41%–90%;

and 3) 91%–100%. As the system generates more snapshots,
 the number of vertices with page utilization between 91% and
 100% decreases significantly.

C. Motivation

This work is strongly motivated by the need to improve
 the traversing performance for the SCM-based evolving graph
 systems by keeping strong graph spatial locality for all
 vertices. We propose a joint management middleware that
 performs both memory allocations and data placements for
 evolving data while taking into account graph spatial locality.
 The major technical challenges are 1) how to maintain strong
 graph spatial locality while the graph evolves, and 2) how to
 intelligently place and rewrite data on SCMs without causing
 excessive energy consumption.

III. SCM-BASED GRAPH-EVOLVING AWARE DATA ARRANGER

A. Overview

This section introduces our SCM-Based GEAR, designed
 to maintain strong graph spatial locality by consolidating
 all neighbors of each vertex on the SCM while minimiz-
 ing energy consumption. Technically, SCM-based GEAR
 serves as middleware between the graph application and
 the SCM device, bridging the information gap between
 them. Implementing GEAR as middleware not only facilitates
 information exchange but also ensures high compatibility,
 avoiding the need to modify either the application or the
 devices. Fig. 4 provides an overview of our design, which
 comprises four key components: 1) multilevel page allocation;
 2) locality-aware data placement; 3) dual-granularity wear
 leveler; and 4) graph updates accumulation.

Our multilevel page allocation component partitions and
 allocates SCM memory areas to store all neighbors associated
 with each vertex. Each vertex’s degree (the number of the
 vertex’s edges) determines the size of its allocated SCM
 memory area. Furthermore, our locality-aware data placement
 mechanism ensures that all evolved graph data (i.e., newly
 updated edges) related to the same source vertex are stored
 in the corresponding SCM memory area, thereby preserving
 strong graph spatial locality. Additionally, our dual-granularity
 wear leveler collaborates with our page allocation strategy to
 evenly distribute graph updates across all memory pages in
 SCM during graph evolution.

³The dataset is from Stanford network analysis project (SNAP) [45].

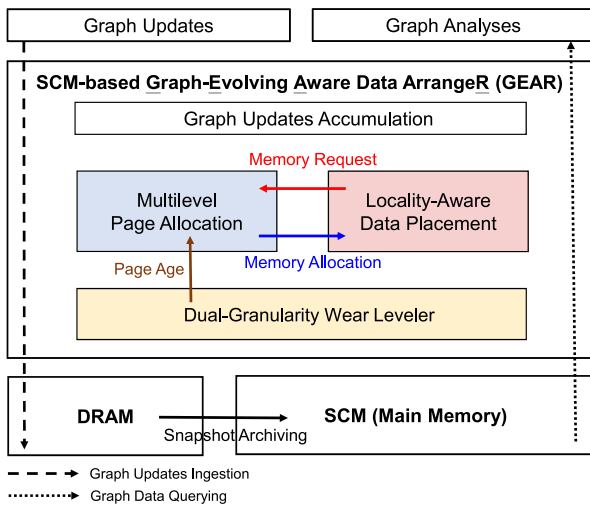


Fig. 4. System architecture.

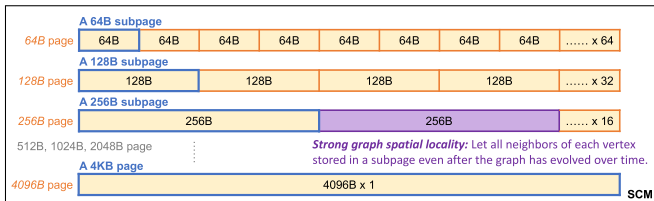


Fig. 5. Example of multilevel page allocation.

Finally, the graph updates accumulation policy buffers incoming graph updates in DRAM. It employs a data structure called an edge log array to facilitate quick querying of these new edges without traversing the entire graph. Because SCM has a higher-write latency than DRAM, our design prioritizes staging new graph updates in DRAM for quick ingestion. The buffered data are subsequently transferred to SCMs in batches, referred to as snapshots. The edge log array maintains incoming graph updates in a first-in-first-out (FIFO) manner, with each update containing three fields: 1) the source vertex; 2) the destination vertex; and 3) the edge weight between them. It is worth noting that such stage-and-flush design is widely used in many graph systems, so we will not go into specific design details.

B. Multilevel Page Allocation

SCM-based GEAR aims to maintain strong graph spatial locality by consolidating all neighbors belonging to each vertex within contiguous memory areas on the SCM. In real-world graphs, hub vertices, which are those with extremely high degrees, have significantly more neighbors than nonhub vertices. Celebrities in social networks are an excellent example of a hub vertice: their graph neighbors can be hundreds, if not thousands, of times more than regular users (nonhub vertices).

Traditionally, most systems allocate memory areas (or pages) of 4 kB. To reduce maintenance costs of graphs evolution, it is common to allocate a 4-kB page for each hub or nonhub vertex. However, this allocation results in low-page utilization. For example, assume that storing one neighbor

edge requires approximately 8 bytes (including the index of the neighbor vertex and the edge weight). Then, storing a nonhub vertex with 100 neighbor edges would only require 800 bytes, well below the 4-kB capacity. Even if the combined neighbors of some hub vertices can fill a 4-kB page, the memory requirement might expand over time and no longer fit within the 4-kB memory area as the graph evolves. A simple solution would be to divide a 4-kB page into smaller sizes, but this would require significant maintenance overhead and result in severe space fragmentation.

The multilevel page allocation strategy in SCM-based GEAR relies on two fundamental principles. First, it aims to minimize maintenance overhead by organizing memory areas into sizes aligned with seven predefined levels (each a power of two in size): 64, 128, 256, 512, 1024, 2048, and 4096 B. To provide a clearer understanding of this concept, Fig. 5 visually illustrates the relationship between a 4-kB page and its potential partitioned levels. For instance, a 4-kB page can be partitioned into 64 64-B subpages, with each subpage dedicated to storing neighbors from the same vertex. Second, the allocation process chooses an appropriate memory area size from among the available options based on the vertex's degree. This adaptive approach ensures that memory allocation is tailored to the each vertex's specific characteristics, resulting in improved performance and resource utilization.

GEAR uses the `mmap` system call to obtain multiple 4-kB pages from the operating system (OS). The multilevel page allocation partitions each 4-kB page into identically sized subpages that fall into one of seven predefined levels. The required size for storing all neighbors associated with a vertex is estimated using the vertex's degree, and a subpage that meets or exceeds this requirement is allocated. This design has a low overhead for multilevel page allocation, requiring only a few extra bits per subpage to find a subpage's location within a 4-kB page. Furthermore, it mitigates the fragmentation issue of fixed-size memory areas. Additionally, the alignment of subpage sizes with the CPU cacheline⁴ (64 B) ensures that unused data is not transferred from SCMs to the CPU cache, thereby optimizing data transfer efficiency.

Fig. 6(a) and (b) show the data structures used by GEAR to manage the mapping between each 4-kB page and its subpages. The page metadata table [Fig. 6(a)] stores all relevant information about each 4-kB page. The granularity flag indicates the size of the corresponding subpage, represented by a 3-bit binary number (for example, a subpage size of 2048 B is denoted as 110). The empty flag indicates whether or not the subpage has been allocated.

The available page lists [Fig. 6(b)] consist of seven arrays, which include a free page list and six size-specific available page lists. The free page list contains all 4-kB pages that have not yet been divided into subpages. Each size-specific available page list corresponds to one of the six subpage levels (64 to 2048 B), maintaining all associated 4-kB pages with unallocated subpages. This design requires only a 4-byte page index to track each page. For example, given a 1-GB SCM,

⁴A cacheline is the smallest unit of data that can be transferred between main memory and the CPU cache.

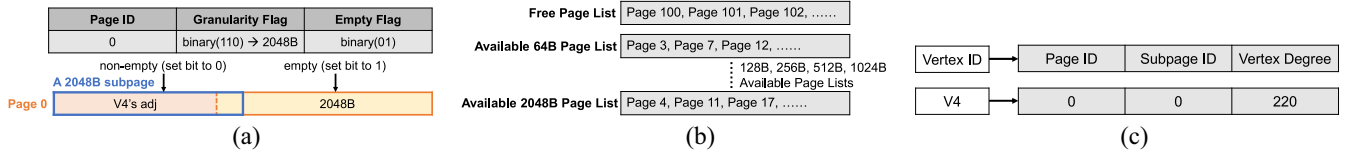


Fig. 6. Data structures for maintaining evolving graph data on SCMs. (a) Page metadata table. (b) Available page list. (c) Vertex-to-page table.

440 there are 262, 144 4-kB pages, and the overall seven arrays
441 consume 1 MB (i.e., 262 and 144 pages \times 4 B).

442 Lastly, GEAR features a vertex-to-page table [Fig. 6(c)] to
443 track the relationship between each vertex and its associated
444 page information. This includes the 1-byte vertex's subpage
445 index, 4-byte page index, and 2-byte vertex degree. Based on
446 our calculations, the combined space overhead of all three data
447 structures (i.e., vertex-to-page table, available page list, and
448 page metadata table) accounts for less than 5% of the total
449 graph size.

450 Let us use an example to demonstrate the page allocation
451 process. To assign a 2048-B subpage to a vertex [e.g., V0 in
452 Fig. 6], the process starts by checking the 2048-B available
453 page list. If it is empty, the system chooses a page from the
454 free page list. The metadata table is then updated, with the
455 granularity flag set to 110 for the selected page, indicating its
456 size as 2048 B. The vertex-to-page table is then updated to
457 associate V0 with the allocated page index, with the subpage
458 index set to 0 and the degree recorded as 220. This allows
459 for efficient management and retrieval of graph data during
460 evolution and traversal.

461 C. Locality-Aware Data Placement

462 The locality-aware data placement strategy aims to maintain
463 strong graph spatial locality while transferring accumulated
464 graph updates from DRAM to SCMs to generate a snap-
465 shot. As part of this strategy, the multilevel page allocation
466 ensures that each vertex's subpage is sufficiently sized⁵ to
467 accommodate all its neighbors. Consequently, each subpage
468 typically contains unused space, known as the reserved area.
469 This reserved area serves as a designated space for future
470 graph updates associated with the vertex, ensuring that new
471 updates to different vertices remain segregated, thus preserving
472 strong graph spatial locality across all vertices.

473 When incorporating a new graph update into a subpage's
474 reserved area, two scenarios may occur: 1) the reserved area
475 of the targeted subpage is either sufficient (i.e., not full) or
476 2) insufficient (i.e., full). If the reserved area is sufficient,
477 graph update is written directly to the appropriate reserved
478 area. In contrast, if the reserved area is insufficient, our
479 approach requires rewriting all previous data within the sub-
480 page, including the entire adjacency list, to a larger subpage.
481 This ensures that the most recent updates are accommodated
482 while preserving strong graph spatial locality for each vertex.
483 Even for node deletion, the graph system generates a new
484 graph update, as explained in Section II-A1. That is, whenever

⁵The size of the subpage must be greater than or equal to the space currently occupied by all neighbors belonging to the vertex.

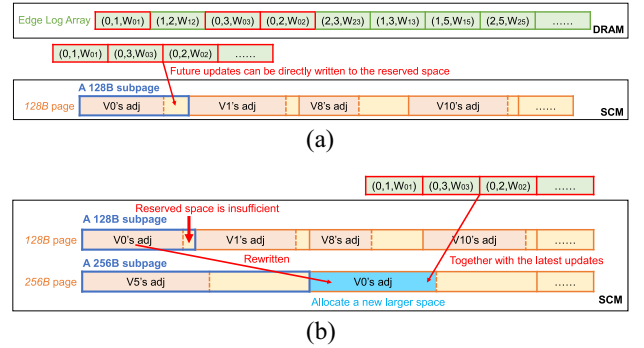


Fig. 7. Two scenarios for the reserved area. (a) Reserved area is not full. (b) Reserved area is full, rewrite data to a larger subpage.

a neighbor is removed from a vertex, a new edge with a
negative value is appended to the adjacency list.

485 For instance, Fig. 7 shows how locality-aware data place-
486 ment works when writing all graph updates associated with
487 source vertex V0 to the SCM. The notation “(0, 1, $W_{0,1}$)”
488 means the edge value between source vertex V0 and its neigh-
489 bor vertex V1 is updated to $W_{0,1}$. There are two cases: when
490 the corresponding reserved area in the SCM is insufficient or
491 sufficient. In both cases, all graph updates are buffered in the
492 edge log array in DRAM. In the case where the reserved area
493 is sufficient, as depicted in Fig. 7(a), our policy directs the
494 writing of all graph updates associated with vertex V0 to the
495 corresponding subpage, which belongs to the 128-B level, in
496 the SCM.
497
498

499 On the other hand, in Fig. 7(b), the reserved area of the
500 subpage associated with vertex V0 lacks enough free space to
501 accommodate graph updates associated with vertex V0. Given
502 that the adjacency list of vertex V0 was originally stored in
503 a 128-B subpage, the data placement mechanism collaborates
504 with the multilevel page allocation to obtain an empty 256-B
505 subpage capable of storing both the old adjacency list and all
506 new updates for vertex V0. Subsequently, the old adjacency
507 list of vertex V0, along with its latest updates from DRAM, is
508 transferred and rewritten to the newly allocated 256-B subpage
509 in the SCM.
510

511 It is important to point out that our strategy only rewrites
512 subpages with insufficient reserved area, rather than rewriting
513 4096-B subpages equivalent to a normal page. Consequently,
514 compared to the merging strategy employed by state-of-the-art
515 frameworks, our strategy achieves strong graph spatial locality
for each vertex with fewer writes.

516 D. Dual-Granularity Wear Leveler

517 Data updates on real-world graphs exhibit a high degree of
518 skew, a phenomenon well-documented in [46], [47], and [48].

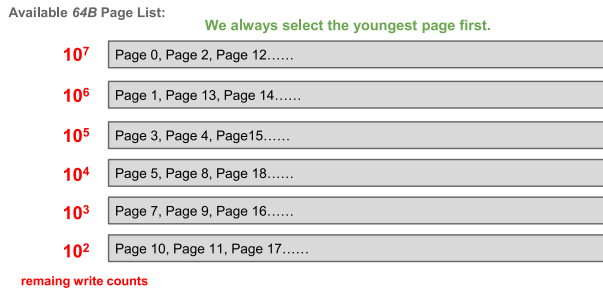


Fig. 8. Interpage wear-leveling mechanism.

519 This skew is primarily attributed to hub vertices that
 520 are densely connected to numerous neighboring vertices.
 521 Consequently, these hub vertices undergo more frequent
 522 updates compared to other vertices. Such skewed updates pose
 523 a significant challenge in the context of SCM, which has
 524 a limited lifetime. Moreover, our design’s manipulation of
 525 subpage allocation introduces a further layer of complexity,
 526 potentially resulting in disparate write counts among subpages
 527 within the same 4-kB memory page. This disparity exacerbates
 528 the wear leveling issue, necessitating a comprehensive
 529 approach to address wear leveling not only across all 4-kB
 530 pages but also within each 4-kB page. To tackle this challenge
 531 comprehensively, we propose a dual-granularity wear leveler
 532 comprising both an interpage wear-leveling mechanism and an
 533 intrapage wear-leveling mechanism.

534 We design the interpage wear-leveling mechanism to ensure
 535 a uniform distribution of write counts across all memory
 536 pages. The main idea is to consistently select the healthier
 537 page during memory allocation. To facilitate this process, we
 538 maintain a per-page write count for each memory page in
 539 the page metadata table, as depicted in Fig. 6(a). Technically,
 540 we use a multilevel page list, where each page list bounds
 541 the minimum remaining write counts for each page within
 542 it. The minimum remaining write count associated with the
 543 highest level is determined based on the ideal lifetime of the
 544 SCM device. To reduce maintenance overhead, we categorize
 545 the minimum remaining write count for each level in an
 546 exponential manner. For example, if an SCM device can
 547 endure at most 10^8 write accesses per cell, our mechanism
 548 configures the page list into six levels: 1) 10^7 ; 2) 10^6 ; 3) 10^5 ;
 549 4) 10^4 ; 5) 10^3 ; and 6) 10^2 , as illustrated in Fig. 8. The number
 550 of each level denotes the minimum remaining write count.
 551 The remaining write count for each page is calculated as 10^8
 552 minus the page write count. For example, 10^7 indicates
 553 that the page belonging to this level can withstand at least
 554 10^7 more write operations. This meticulous categorization
 555 ensures an even distribution of write operations across memory
 556 pages, thereby effectively mitigating wear-leveling issues at
 557 the interpage level.

558 As detailed in Section III-C, insufficient space in a subpage
 559 designated for storing graph updates the rewriting of all data
 560 from the original subpage to a larger subpage. Such movement
 561 of vertices between subpages within the same 4-kB page
 562 can lead to wear-unleveling issues. To address this concern,
 563 we introduce an intrapage wear-leveling mechanism, which

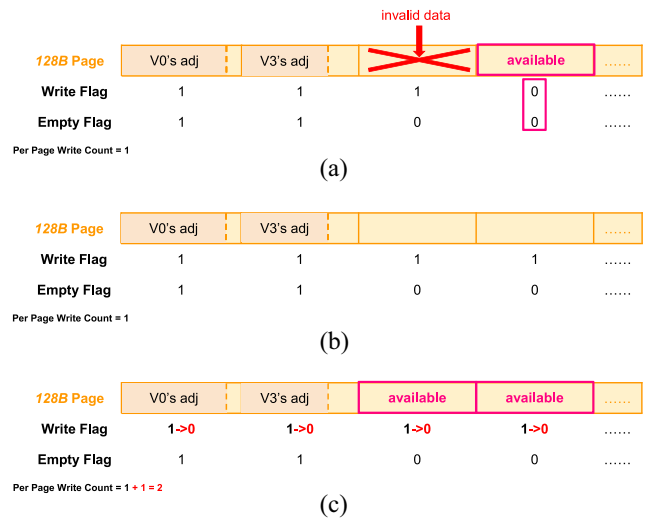


Fig. 9. Intrapage wear-leveling mechanism. (a) Available page: Write flag == 0 and empty flag == 0. (b) No available page. (c) Reset write flag and per page write count + 1.

is implemented by maintaining a 1-bit write flag and a 1-bit
 empty flag in the page metadata table for each subpage. The
 write flag records whether the subpage has been written in the
 current round, with 1 indicating that it has been written and
 0 indicating otherwise. Additionally, the empty flag denotes
 whether the subpage is currently used by a vertex’s adjacency
 list, with 1 indicating used and 0 indicating availability.

As shown in Fig. 9(a), we only allocate a subpage when
 both the write flag and empty flag are 0, to ensure balanced
 write counts across all subpages within the same 4-kB page.
 When none of the pages in the available page list have
 available subpages, it indicates most of the subpages in these
 pages were written during this round. Thus, we reset all
 the write flags of the available page list to 0 and increment
 the per-page write count by 1. Subsequently, all subpages
 become available again, as depicted in Fig. 9(b) and (c).
 This approach not only maximizes the utilization of available
 subpages but also ensures the amortization of write counts
 across all subpages within the same 4-kB page, effectively
 mitigating wear leveling issues at the intrapage level.

IV. PERFORMANCE EVALUATION

A. Evaluation Setup and Performance Metrics

This section evaluates the efficacy of GEAR in enhancing
 the performance of both graph traversal and graph evolution.
 We thoroughly compared SCM-based GEAR to three baseline
 approaches, checking their performance in a number of areas,
 such as execution time, TLB miss rate, CPU cache miss
 rate, energy use, and the number of writes to the SCM.
 The three baseline approaches consist of two state-of-the-art
 evolving graph processing frameworks: 1) LLAMA [21], con-
 figured with merge frequencies set to 100 and 500 snapshots
 and 2) GraphOne [23], which incorporates cache-line-sized
 memory allocation and hub vertex handling. GraphOne’s
 memory allocation strategy provides a cache-line-sized (i.e.,
 64 bytes) area for storing nonhub vertices, while its hub vertex

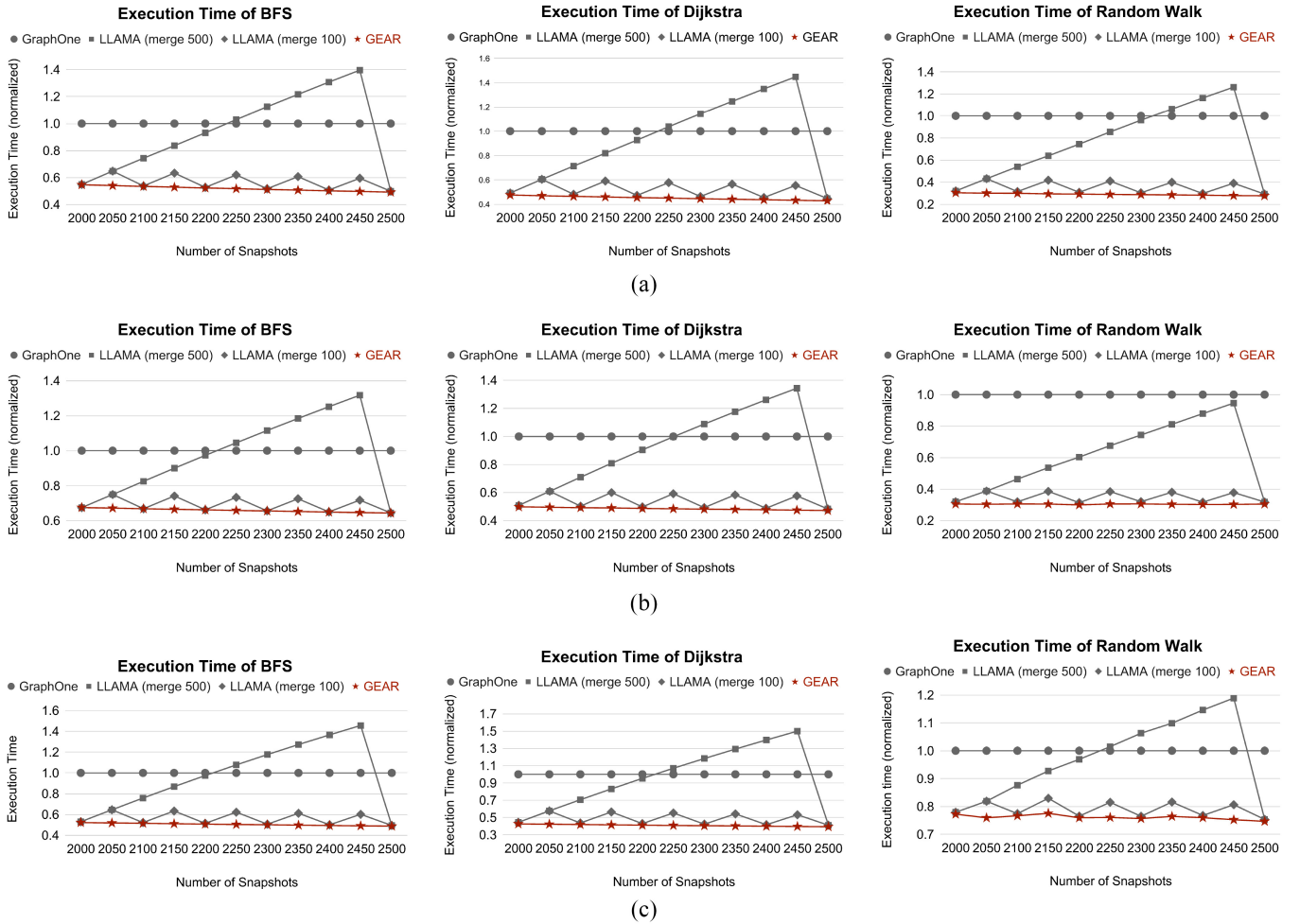


Fig. 10. Normalized execution time of running graph algorithms on evolving graphs. (a) Dataset: Orkut. (b) Dataset: Twitter-2010. (c) Dataset: Friendster.

599 handling allocates a 4-kB page to accommodate all edges
 600 belonging to a hub vertex. It is noteworthy that, according to
 601 the literature, GraphOne includes delta checkpointing similar
 602 to LLAMA, but GraphOne does not enable checkpointing by
 603 default. Without loss of generality, all of the three baseline
 604 approaches place frequently accessed data in DRAM and less
 605 frequently accessed data in SCM.

606 To ensure a comprehensive evaluation, we selected three
 607 representative datasets from the SNAP [45]: 1) Orkut;
 608 2) Twitter-2010; and 3) Friendster. The Orkut dataset encom-
 609 passes 3 million vertices and 0.23 billion edges. The Twitter
 610 2010 dataset comprises 40 million vertices and 1.5 billion
 611 edges. Lastly, the Friendster dataset includes 56 million
 612 vertices and 2.6 billion edges. We selected these datasets to
 613 offer a wide variety of graph sizes and complexities, enabling
 614 a thorough assessment of the performance of SCM-based
 615 GEAR.

616 We segment each graph dataset into 10 000 snapshots to
 617 simulate the graph evolution process. We execute three widely
 618 used graph traversal algorithms—breadth-first search (BFS),
 619 Dijkstra (single source shortest path algorithm), and Random
 620 Walk algorithms—on the evolving graph at intervals of
 621 100 snapshots. We capture memory traces during the traversal
 622 and subsequently replay them on our trace-based simulator.
 623 Our simulator simulates an Intel Skylake architecture with

a fully associative TLB comprising 1536 entries and an 8
 624 MB, 16-way associative L3 cache [49], [50]. The read/write
 625 latency for DRAM and SCMs is set to 50/50 and 120/150
 626 ns, respectively, based on previous studies [6]. Additionally, it
 627 accounts for the energy consumption associated with writing
 628 a bit to the SCM, estimated at 16.82 pJ per bit [51]. The
 629 simulation environment is hosted on a server featuring an Intel
 630 Xeon Gold 6252n CPU, 768 GB of DRAM, and running Linux
 631 kernel version 5.4. This setup ensures a realistic emulation
 632 of the graph traversal algorithms' performance under various
 633 evolving graph scenarios, enabling a thorough evaluation of
 634 SCM-based GEAR and baseline strategies.
 635

B. Evaluation Results 636

637 1) *Performance Evaluation of Graph Traversal:* In this
 638 section, we focus on demonstrating the performance of
 639 traversing an evolved graph. Unlike graph evolution, graph
 640 traversal does not require additional data writes and therefore
 641 does not impact the system's lifetime. Fig. 10(c) presents the
 642 results of the total execution time when running SCM-based
 643 GEAR against the three baseline approaches. Specifically,
 644 Fig. 10(a) and (b) depict the results obtained from executing
 645 traversal algorithms on the Twitter-2010 and Friendster
 646 datasets, respectively. The x -axis of each figure represents the number

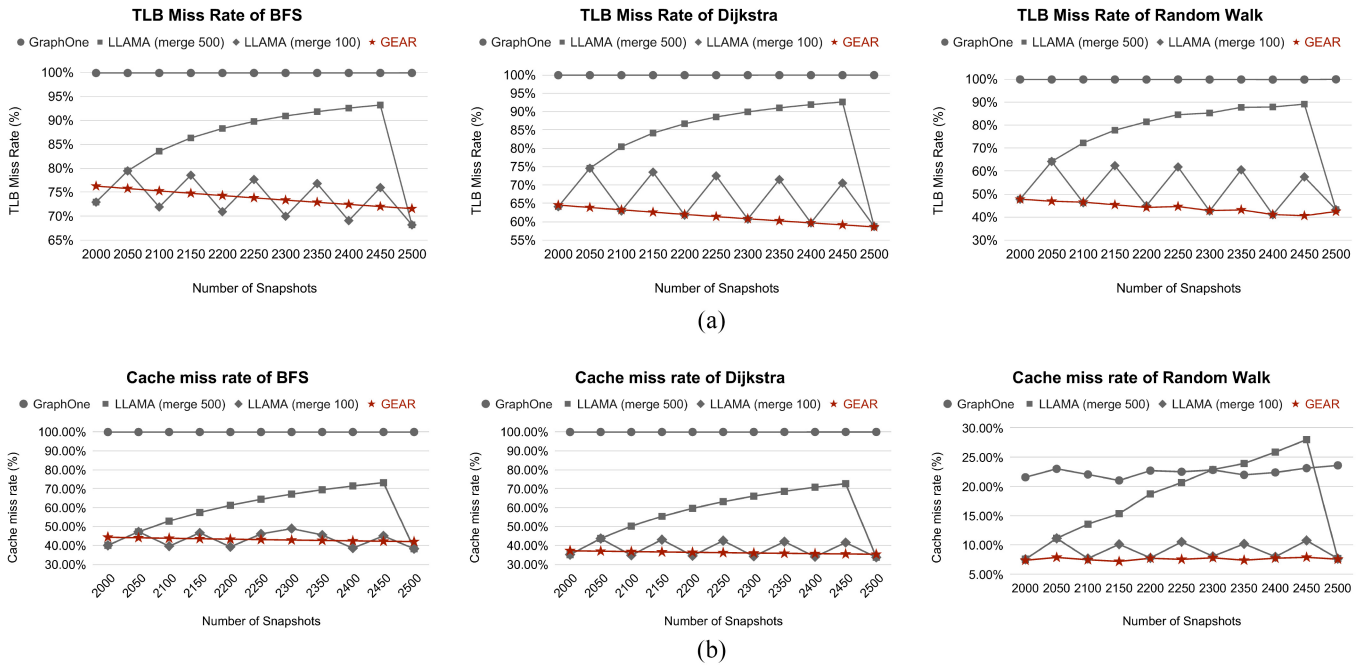


Fig. 11. TLB and CPU cache miss rate of running graph traversal algorithms (DataSet: Friendster). (a) TLB miss rate. (b) CPU cache miss rate.

of archived snapshots, while the y-axis displays the execution time normalized to that of GraphOne. Due to the similarity in performance trends across all 10000 archived snapshots, we only present results for the interval between 2000 and 2500 archived snapshots.

The results reveal that SCM-based GEAR achieves execution time savings ranging from 23% to 70% compared to GraphOne, 0% to 74% compared to LLAMA (merge 500), and 0% to 27% compared to LLAMA (merge 100). These savings are attributed to SCM-based GEAR’s ability to maintain strong graph spatial locality, leading to fewer TLB misses when accessing pages during graph traversal. Notably, SCM-based GEAR achieves an execution time reduction comparable to LLAMA, especially when the graph algorithm executes immediately after LLAMA triggers snapshot merging. However, LLAMA’s performance may exhibit instability, and frequent snapshot merging, such as every 100 snapshots, can lead to excessive energy consumption (further details are provided in Section IV-B2).

To provide a detailed breakdown evaluation, Fig. 11 shows cases the TLB miss rate and CPU cache miss rate results obtained when running SCM-based GEAR against the three baseline approaches on the Friendster dataset. In each figure, the x-axis represents the number of archived snapshots, while the y-axis depicts the TLB miss rate in Fig. 11(a) and the CPU cache miss rate in Fig. 11(b). It is evident from the figures that SCM-based GEAR consistently maintains a relatively low TLB miss rate and CPU cache miss rate across all numbers of snapshots. Conversely, the TLB miss rate and CPU cache miss rate observed in systems running GraphOne and LLAMA exhibit fluctuations, occasionally exceeding 90% (except the CPU cache miss rate caused by running a random walk), depending on the number of snapshots created. GraphOne experiences exceptionally high-TLB miss rates and CPU cache miss rates due to the absence of a snapshot merging strategy

to preserve graph spatial locality during graph evolution. In contrast, LLAMA (merge 500) achieves relatively low-TLB miss rates and CPU cache miss rates every 500 snapshots when the snapshot merging strategy is executed, but the rate steadily increases to around 90%. Employing LLAMA with frequent snapshot merging, such as LLAMA (merge 100), can mitigate the occurrence of excessively high-TLB miss rates. However, the frequent merging strategy significantly prolongs the graph evolution process and, even worse, adversely affects the SCM’s lifespan. More detailed evaluations of evolving time and memory endurance will be presented in the subsequent subsections.

2) *Performance and Lifetime Evaluation of Graph Evolution:* Fig. 12 presents a comprehensive evaluation of both the performance and lifetime aspects of graph evolution. In Fig. 12(a), the time taken to evolve the graph to a specific number of snapshots using different approaches is depicted. The x-axis ranges from 1000 to 6000, representing the number of snapshots, while the y-axis indicates the time for graph evolution normalized to GraphOne. The evaluation shows that systems running SCM-based GEAR exhibit superior evolving performance compared to LLAMA due to GEAR’s lower-time complexity. Conversely, LLAMA incurs greater time consumption due to the periodic merging of snapshots, necessitating the rewriting of all snapshots. For example, LLAMA (merge 100) causes a longer graph evolution time than LLAMA (merge 500) because snapshot merging is triggered more frequently. Furthermore, SCM’s high-write latency contributes to the extended time required for graph evolution.

For a more detailed analysis of the graph evolution performance, Fig. 12(b) illustrates the total edge write counts to SCM for each system at intervals of 50 snapshots between 2000 and 2500 snapshots. The x-axis represents the number of archived snapshots, while the y-axis indicates the total edge

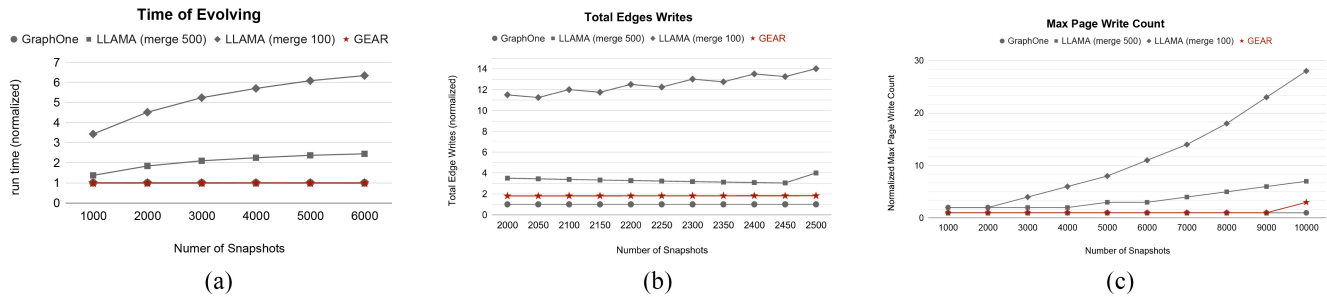


Fig. 12. Performance and lifetime evaluation on evolving a graph. (a) Time spent evolving the graph (DataSet: twitter). (b) Total number of edge writes. (c) Maximum write counts among all pages.

717 writes normalized to GraphOne. GraphOne, which does not
 718 incorporate snapshot merging in our experiments, does not
 719 generate extra writes. In contrast, SCM-based GEAR may
 720 produce more edge writes than GraphOne if the reserved
 721 space of a vertex is insufficient, leading to the rewriting
 722 of the original adjacency list to a newly allocated larger
 723 subpage along with the latest updates. However, because the
 724 SCM-based GEAR only rewrites vertices with inadequate
 725 reserved space and limits the maximum rewriting size to 2048
 726 bytes, its total edge writes are only about 2.1 times higher
 727 than GraphOne’s. Importantly, GEAR’s total edge writes are
 728 significantly lower than those of LLAMA, which merges
 729 snapshots on a regular basis.

730 While LLAMA may achieve faster graph traversal by
 731 merging snapshots more frequently, this has a significant
 732 impact on SCM’s lifespan. Fig. 12(c) illustrates the normalized
 733 maximum page write count as the system generates snapshots
 734 ranging from 1000 to 10 000. The x -axis denotes the number
 735 of snapshots, while the y -axis represents the maximum page
 736 write count normalized to GraphOne. The results demonstrate
 737 that our dual-granularity wear leveler is effective in mitigating
 738 the increase in maximum page write count. This effectiveness
 739 stems from the distribution of writes to a finer granularity,
 740 specifically at the subpage level. Conversely, when LLAMA
 741 frequently merges snapshots, the maximum page write count
 742 experiences a sharp escalation, as observed in the case of
 743 LLAMA (merge 100).

744 3) *Evaluation on Energy Consumption:* We further evalu-
 745 ate the energy consumption associated with different graph
 746 evolution approaches, as depicted in Fig. 13. The x -axis rep-
 747 resents the number of snapshots ranging from 1000 to 10 000,
 748 while the y -axis indicates the energy consumption. Each plot
 749 in the figure illustrates the cumulative energy consumption
 750 required to execute the total number of snapshots indicated on
 751 the x -axis. Fig. 13 highlights that SCM-based GEAR exhibits
 752 relatively low-energy consumption compared to LLAMA.
 753 This is primarily because the rewrite operations triggered by
 754 SCM-based GEAR result in fewer write accesses on SCMs
 755 compared to the merging operations triggered by LLAMA.
 756 Notably, GraphOne, which does not perform any snapshot
 757 merging operations, consumes the least energy among all
 758 solutions. Although SCM-based GEAR consumes more energy
 759 than GraphOne, its scalability remains intact. This is evidenced
 760 by the consistent energy consumption gap between GraphOne
 761 and SCM-based GEAR, even as the graph evolves over time.

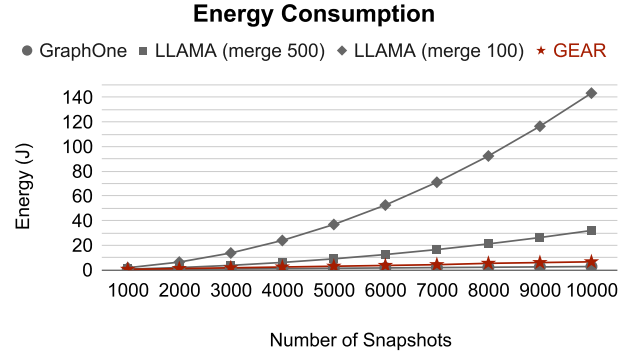


Fig. 13. Energy consumption (Dataset: Friendster).

In contrast, LLAMA’s energy consumption exhibits a linear 762
 increase as the graph evolves, making it nonscalable. For 763
 instance, LLAMA (merge 100) consumes 3 and 21 times more 764
 energy than SCM-based GEAR when there are 1000 snapshots 765
 and 10 000 snapshots, respectively. 766

V. CONCLUSION 767

768 Our research addresses the challenge of weak graph spatial 768
 locality in evolving graph frameworks, which hinders efficient 769
 execution of graph traversal algorithms. To mitigate this 770
 issue, we introduce SCM-Based GEAR, a joint management 771
 middleware that optimizes the arrangement and storage of 772
 evolving graph data in both DRAM and SCMs. GEAR 773
 comprises multilevel page allocation, locality-aware data 774
 placement, and dual-granularity wear leveling components. 775
 GEAR improves graph traversal performance while maintaining 776
 strong graph spatial locality as the graph changes. It does this by 777
 allocating subpages based on vertex-neighboring relationships, 778
 keeping unused areas for future updates, and evenly spreading 779
 write operations. Our evaluation demonstrates the effectiveness 780
 of SCM-based GEAR, showing significant improvements in 781
 execution time savings ranging from 23% to 70% compared to 782
 state-of-the-art frameworks. Through meticulous management 783
 of evolving graph data across memory devices, GEAR achieves 784
 superior performance in traversing evolving graphs, addressing 785
 critical challenges posed by weak graph spatial locality. 786

REFERENCES 787

- [1] C.-F. Wu, C.-J. Wu, G.-Y. Wei, and D. Brooks, “A joint management 788
 middleware to improve training performance of deep recommendation 789
 systems with SSDs,” in *Proc. 59th ACM/IEEE Design Autom. Conf.*, 790
 2022, pp. 157–162. 791

- [2] W. Fan et al., “Graph neural networks for social recommendation,” in *Proc. World Wide Web Conf.*, 2019, pp. 417–426.
- [3] J. Leskovec, J. Kleinberg, and C. Faloutsos, “Graph evolution: Density and shrinking diameters,” *ACM Trans. Knowl. Discov. Data*, vol. 1, no. 1, p. 2, 2007.
- [4] G. Dhiman, R. Ayoub, and T. Rosing, “PDRAM: A hybrid PRAM and DRAM main memory system,” in *Proc. 46th Annu. Design Autom. Conf.*, 2009, pp. 664–669.
- [5] Y.-C. Chen, C.-F. Wu, Y.-H. Chang, and T.-W. Kuo, “Exploring synchronous page fault handling,” *IEEE Trans. Comput.-Aided Design Integr. Circuits Syst.*, vol. 41, no. 11, pp. 3791–3802, Nov. 2022.
- [6] C.-F. Wu, Y.-H. Chang, M.-C. Yang, and T.-W. Kuo, “Joint management of CPU and NVDIMM for breaking down the great memory wall,” *IEEE Trans. Comput.*, vol. 69, no. 5, pp. 722–733, May 2020.
- [7] C. J. Xue, G. Sun, Y. Zhang, J. J. Yang, Y. Chen, and H. Li, “Emerging non-volatile memories: Opportunities and challenges,” in *Proc. 7th IEEE/ACM/IFIP Int. Conf. Hardw./Softw. Codesign Syst. Synth.*, 2011, pp. 325–334.
- [8] B. Van Essen, H. Hsieh, S. Ames, R. Pearce, and M. Gokhale, “DI-MMAP—A scalable memory-map runtime for out-of-core data-intensive applications,” *Clust. Comput.*, vol. 18, pp. 15–28, Mar. 2015.
- [9] J. Zhang et al., “Revamping storage class memory with hardware automated memory-over-storage solution,” in *Proc. ACM/IEEE 48th Annu. Int. Symp. Comput. Archit. (ISCA)*, 2021, pp. 762–775.
- [10] S. Brin and L. Page, “The anatomy of a large-scale hypertextual Web search engine,” *Comput. Netw. ISDN Syst.*, vol. 30, nos. 1–7, pp. 107–117, 1998.
- [11] A. Ching, S. Edunov, M. Kabiljo, D. Logothetis, and S. Muthukrishnan, “One trillion edges: Graph processing at Facebook-scale,” *Proc. VLDB Endowment*, vol. 8, no. 12, pp. 1804–1815, 2015.
- [12] M. Zhang, Y. Wu, Y. Zhuo, X. Qian, C. Huan, and K. Chen, “Wonderland: A novel abstraction-based out-of-core graph processing system,” *ACM SIGPLAN Notices*, vol. 53, no. 2, pp. 608–621, 2018.
- [13] Z. Ai, M. Zhang, Y. Wu, X. Qian, K. Chen, and W. Zheng, “Squeezing out all the value of loaded data: An out-of-core graph processing system with reduced disk I/O,” in *Proc. USENIX Annu. Tech. Conf. (USENIX ATC)*, 2017, pp. 125–137.
- [14] A. Kyrola, G. Blelloch, and C. Guestrin, “GraphChi: Large-scale graph computation on just a PC,” in *Proc. 10th USENIX Symp. Oper. Syst. Design Implement. (OSDI)*, 2012, pp. 31–46.
- [15] D. Zheng, D. Mhembere, R. Burns, J. Vogelstein, C. E. Priebe, and A. S. Szalay, “FlashGraph: Processing billion-node graphs on an array of commodity SSDs,” in *Proc. 13th USENIX Conf. File Storage Technol. (FAST)*, 2015, pp. 45–58.
- [16] H. Liu and H. H. Huang, “Graphene: Fine-grained I/O management for graph computing,” in *Proc. 15th USENIX Conf. File Storage Technol. (FAST)*, 2017, pp. 285–300.
- [17] K. K. Matam, G. Koo, H. Zha, H.-W. Tseng, and M. Annavaram, “GraphSSD: Graph semantics aware SSD,” in *Proc. 46th Int. Symp. Comput. Archit.*, 2019, pp. 116–128.
- [18] R. Kumar, J. Novak, and A. Tomkins, “Structure and evolution of online social networks,” in *Proc. 12th ACM SIGKDD Int. Conf. Knowl. Discov. Data Min.*, 2006, pp. 611–617.
- [19] T. Yang, Y. Chi, S. Zhu, Y. Gong, and R. Jin, “Detecting communities and their evolutions in dynamic social networks—A Bayesian approach,” *Mach. Learn.*, vol. 82, pp. 157–189, Feb. 2011.
- [20] A. P. Iyer, L. E. Li, T. Das, and I. Stoica, “Time-evolving graph processing at scale,” in *Proc. 4th Int. Workshop Graph Data Manag. Exp. Syst.*, 2016, pp. 1–6.
- [21] P. Macko, V. J. Marathe, D. W. Margo, and M. I. Seltzer, “LLAMA: Efficient graph analytics using large multiversioned arrays,” in *Proc. IEEE 31st Int. Conf. Data Eng.*, 2015, pp. 363–374.
- [22] U. Khurana and A. Deshpande, “Efficient snapshot retrieval over historical graph data,” in *Proc. IEEE 29th Int. Conf. Data Eng. (ICDE)*, 2013, pp. 997–1008.
- [23] P. Kumar and H. H. Huang, “GraphOne: A data store for real-time analytics on evolving graphs,” *ACM Trans. Storage (TOS)*, vol. 15, no. 4, pp. 1–40, 2020.
- [24] Y. Jin, C.-F. Wu, D. Brooks, and G.-Y. Wei, “S³: Increasing GPU utilization during generative inference for higher throughput,” in *Proc. Adv. Neural Inf. Process. Syst.*, 2023, pp. 18015–18027.
- [25] F. T. Hady, A. Foong, B. Veal, and D. Williams, “Platform storage performance with 3D XPoint technology,” *Proc. IEEE*, vol. 105, no. 9, pp. 1822–1833, Sep. 2017.
- [26] O. Krestinskaya, A. P. James, and L. O. Chua, “Neuromemristive circuits for edge computing: A review,” *IEEE Trans. Neural Netw. Learn. Syst.*, vol. 31, no. 1, pp. 4–23, Jan. 2020.
- [27] K. Wu, A. C. Arpaci-Dusseau, and R. H. Arpaci-Dusseau, “Towards an unwritten contract of Intel Optane SSD,” in *Proc. 11th USENIX Workshop Hot Topics Storage File Syst. (HotStorage)*, 2019, pp. 1–8.
- [28] C.-F. Wu, M.-C. Yang, Y.-H. Chang, and T.-W. Kuo, “Hot-spot suppression for resource-constrained image recognition devices with nonvolatile memory,” *IEEE Trans. Comput.-Aided Design Integr. Circuits Syst.*, vol. 37, no. 11, pp. 2567–2577, Nov. 2018.
- [29] W. Cheong et al., “A flash memory controller for 15μs ultra-low-latency SSD using high-speed 3D NAND flash with 3μs read time,” in *Proc. IEEE Int. Solid-State Circuits Conf. (ISSCC)*, 2018, pp. 338–340.
- [30] J. Zhang et al., “FlashShare: Punching through server storage stack from kernel to firmware for ultra-low latency SSDs,” in *Proc. 13th USENIX Symp. Oper. Syst. Design Implement. (OSDI 18)*, 2018, pp. 477–492.
- [31] C.-F. Wu, Y.-H. Chang, M.-C. Yang, and T.-W. Kuo, “When storage response time catches up with overall context switch overhead, what is next?” *IEEE Trans. Comput.-Aided Design Integr. Circuits Syst.*, vol. 39, no. 11, pp. 4266–4277, Nov. 2020.
- [32] C.-F. Wu, Y.-H. Chang, M.-C. Yang, and T.-W. Kuo, “How to steal CPU idle time when synchronous I/O mode becomes promising,” in *Proc. 61th ACM/IEEE Design Autom. Conf. (DAC)*, 2024.
- [33] R. F. Freitas and W. W. Wilcke, “Storage-class memory: The next storage system technology,” *IBM J. Res. Develop.*, vol. 52, no. 4.5, pp. 439–447, Jul. 2008.
- [34] G. W. Burr, B. N. Kurdi, J. C. Scott, C. H. Lam, K. Gopalakrishnan, and R. S. Shenoy, “Overview of candidate device technologies for storage-class memory,” *IBM J. Res. Develop.*, vol. 52, no. 4.5, pp. 449–464, Jul. 2008.
- [35] (Intel, Santa Clara, CA, USA). *Product: Intel Optane Persistent Memory (DCPMM)*. (2020). [Online]. Available: <https://www.intel.com/content/www/us/en/products/docs/memory-storage/optane-persistent-memory/overview.html>
- [36] A. Sainio et al. “NVDIMM: Changes are here so what’s next: Memory computer summit.” 2016. [Online]. Available: <https://www.snia.org/sites/default/files/SSSI/NVDIMM>
- [37] M. Saxena and M. M. Swift, “FlashVM: Virtual memory management on flash,” in *Proc. USENIX Annu. Tech. Conf. (USENIX ATC)*, 2010, pp. 1–14.
- [38] S. Van Doren, “HOTI 2019: Compute express link,” in *Proc. IEEE Symp. High-Perform. Interconnects (HOTI)*, 2019, p. 18.
- [39] D. D. Sharma, “Compute express link (CXL): Enabling heterogeneous data-centric computing with heterogeneous memory hierarchy,” *IEEE Micro*, vol. 43, no. 2, pp. 99–109, Mar./Apr. 2023.
- [40] M. Jung, “Hello bytes, bye blocks: PCIe storage meets compute express link for memory expansion (CXL-SSD),” in *Proc. 14th ACM Workshop Hot Topics Storage File Syst.*, 2022, pp. 45–51.
- [41] H. Li et al., “Pond: CXL-based memory pooling systems for cloud platforms,” in *Proc. 28th ACM Int. Conf. Archit. Support Program. Lang. Oper. Syst.*, 2023, pp. 574–587.
- [42] I. Oukid, J. Lasperas, A. Nica, T. Willhalm, and W. Lehner, “FPTree: A hybrid SCM-DRAM persistent and concurrent B-tree for storage class memory,” in *Proc. Int. Conf. Manag. Data*, 2016, pp. 371–386.
- [43] H.-Y. Cheng et al., “Future computing platform design: A cross-layer design approach,” in *Proc. Design, Autom. Test Eur. Conf. Exhib. (DATE)*, 2021, pp. 312–317.
- [44] I. Oukid, D. Booss, A. Lespinasse, W. Lehner, T. Willhalm, and G. Gomes, “Memory management techniques for large-scale persistent-main-memory systems,” *Proc. VLDB Endowment*, vol. 10, no. 11, pp. 1166–1177, 2017.
- [45] J. Leskovec et al., “Stanford network analysis project.” 2010. [Online]. Available: <https://snap.stanford.edu/>
- [46] T.-S. Lo, C.-F. Wu, Y.-H. Chang, T.-W. Kuo, and W.-C. Wang, “Space-efficient graph data placement to save energy of ReRAM crossbar,” in *Proc. IEEE/ACM Int. Symp. Low Power Electron. Design (ISLPED)*, 2021, pp. 1–6.
- [47] R. Chen, J. Shi, Y. Chen, B. Zang, H. Guan, and H. Chen, “PowerLyra: Differentiated graph computation and partitioning on skewed graphs,” *ACM Trans. Parallel Comput.*, vol. 5, no. 3, pp. 1–39, 2019.
- [48] J. E. Gonzalez, Y. Low, H. Gu, D. Bickson, and C. Guestrin, “PowerGraph: Distributed graph-parallel computation on natural graphs,” in *Proc. 10th USENIX Symp. Oper. Syst. Design Implement. (OSDI)*, 2012, pp. 17–30.
- [49] P. Vila, B. Köpf, and J. F. Morales, “Theory and practice of finding eviction sets,” in *Proc. IEEE Symp. Security Privacy (SP)*, 2019, pp. 39–54.
- [50] J. H. Ryoo, N. Guler, S. Song, and L. K. John, “Rethinking TLB designs in virtualized environments: A very large part-of-memory TLB,” *ACM SIGARCH Comput. Archit. News*, vol. 45, no. 2, pp. 469–480, 2017.
- [51] B. C. Lee, E. Ipek, O. Mutlu, and D. Burger, “Architecting phase change memory as a scalable dram alternative,” in *Proc. 36th Annu. Int. Symp. Comput. Archit.*, 2009, pp. 2–13.